

IDENTIFIABILITY OF THE SPATIAL SEIR-HCD MODEL OF COVID-19 PROPAGATION*

Olga Krivorotko^{1,2a}, Tatiana Zvonareva^{2b}, Andrei Neverov^{2c}

¹Yugra University, Khanty-Mansiysk, 628012 Russia,

²Sobolev Institute of Mathematics SB RAS, Novosibirsk, 630090 Russia

e-mail: ^akrivorotko.olya@mail.ru, ^bt.zvonareva@g.nsu.ru, ^ca.neverov@g.nsu.ru

This paper investigates the identifiability of a spatial mathematical model of the spread of fast-moving epidemics based on the law of acting masses and diffusion processes. The research algorithm is based on global methods of Sobol sensitivity analysis and Bayesian approach, which together allowed to reduce the variation boundaries of unknown parameters for further solving the problem of parameter identification by measurements of the number of detected cases, critical and dead. It is shown that for identification of diffusion coefficients responsible for the rate of movement of individuals in space, it is necessary to use additional information about the process.

Keywords: reaction-diffusion model, identifiability, sensitivity analysis, source problem, optimization.

INTRODUCTION

Mathematical modelling of the spread of infectious diseases has come a long way with the outbreak of a new coronavirus infection caused by SARS-CoV-2 virus in 2019 in Wuhan. From classical differential models of epidemiology, whose foundation was laid in the work of Kermack and McKendrick in 1927 [1], to agent-based models and mean-field control models, as well as their combination, researchers are still faced with incomplete and inaccurate data to sustainably describe the spread of epidemics. A more comprehensive review of models of fast-moving epidemic spread is given in the paper [2] and summarized in the figure 1.

This paper investigates the direct and inverse problem for a spatial SEIR-HCD model of COVID-19 propagation in the region [3]:

$$\frac{\partial u}{\partial t} = \nabla(nv\nabla u) + f(u, q), \quad u(x,0) = u_0(x), \quad t \in (0, T). \quad (1)$$

Here $u(x,t) = (s, e, i, r, h, c, d)(x,t)$ is the vector of system states characterizing the densities of susceptible (s), asymptomatic infected (e), COVID-19 patients (i), recovered (r), hospitalized (h), critical cases requiring ALV device connection (c) and died (d) as a result of COVID-19. The parameters $v = (v_s, v_e, v_i, v_r)$ and $q(x) \in C(\mathbb{R}^m)$ are continuous spatial functions that describe the rate of movement of the respective populations in space and the patterns of infection in the population, respectively. Without limiting generality, we will consider a dimensionless one-dimensional space on x , i. e., $x \in (0,1)$.

The mathematical model (1) is based on a mass balance law in which the entire modelled population is constant in time, i. e. $n(x,t) = n(x)$, where

$$n(x,t) = s(x,t) + e(x,t) + i(x,t) + r(x,t) + h(x,t) + c(x,t) + d(x,t).$$

For the first time in 1937, A. N. Kolmogorov, I. G. Petrovsky and N. S. Piskunov [4] proposed and justified the mathematical model (1), which later became known as the reaction-diffusion model, and also strictly proved that if the initial condition satisfies the following restrictions

$$0 \leq u(x,0) \leq 1, \quad u(x,0) = 0 \quad \forall x < x_1 \quad \text{and} \quad u(x,0) = 1 \quad \forall x > x_2 \geq x_1,$$

*The research was carried out within the state assignment of Ministry of Science and Higher Education of the Russian Federation (theme № FENG-2023-0004, “Analytical and numerical study of inverse problems on recovering parameters of atmosphere or water pollution sources and (or) parameters of media”).

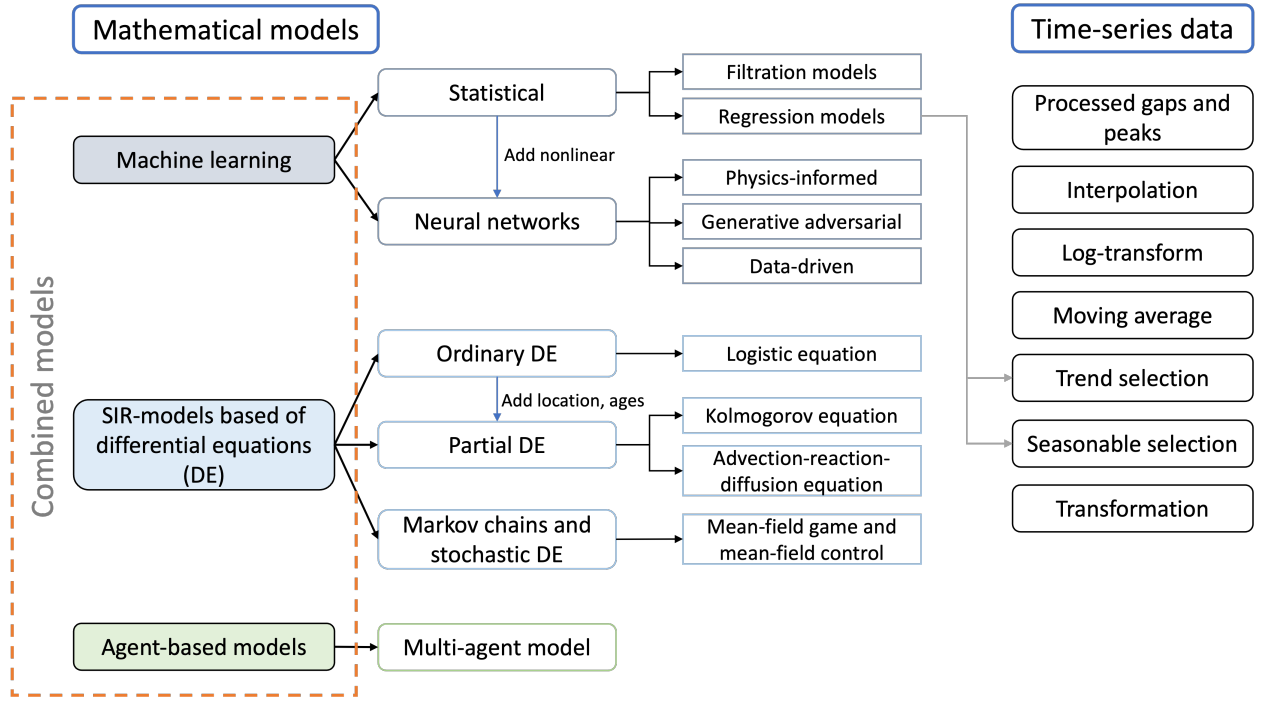


Figure 1: Brief review of mathematical models of epidemic spread and relationship to statistical approaches.

then for $f(u) = u(1 - u)$ the population dynamics in time is described by the rate $v^* = 2\sqrt{f'(0)nv}$. It is interesting to note that similar wave solutions are found in the distributed epidemic propagation model [5]. In the above situation, such oscillatory solutions are interpreted as repeated outbreaks of epidemics.

Taking spatial heterogeneity into account makes it possible to more accurately model an epidemic from a spreading center (a large city in a country, a capital city in a region, etc.) under known initial conditions. Thus, in [6–9], estimates of the spread of COVID-19 in the first months of the epidemic, taking into account passenger traffic, were obtained. In [10], the authors propose a multiscale spatial model based on a system of SEIR-type kinetic transport equations describing the passenger population moving at large scales (outside the city) and a system of diffusion equations describing the urban population acting at small scales. This modelling approach avoids unrealistic effects of traditional diffusion models in epidemiology, such as infinite diffusion rates at large scales and mass migration dynamics. The system parameters include both epidemiological characteristics (number of contacts, disease rate) and socioeconomic characteristics (social distance, vaccination). Given empirically defined parameters, the authors obtained the spatial distribution of the COVID-19 epidemic in Italy by solving systems of partial derivative equations using the finite volume method on unstructured meshes. In [11], an integro-differential equation with delay describing the epidemic spreading process is proposed and studied, in which the solution has some biologically valid features. The feature of epidemiological models consists of the principle of transmission from an infected I to a susceptible S individual, which is characterized by the type of function $f(u, q)$, i. e. the function

$$f_I(S, I, q) = \frac{\beta(x)SI^p}{1 + \kappa I}$$

characterizes the non-linear transmission of viral infection with a number of contacts $\beta(x)$ and a parameter $\kappa > 0$ describing social distance or other socioeconomic constraints during the period of infection spread.

The paper is organized as follows. In section 1, the formulation of the SEIR-HCD model, its spatial interpretation, and methods for its numerical solution are introduced. In section 2, the formulation of the inverse problem for the spatial SEIR-HCD model is presented. Sensitivity

analyses by two global methods are carried out in section 2.2. The algorithm for the numerical solution of the inverse problem, taking into account the identifiability results, is described in 3.

1. DIRECT PROBLEM FORMULATION FOR THE SPATIAL SEIR-HCD MODEL

In [12], a mathematical model of the COVID-19 outbreak propagation, based on the mass balance law and described by a system of 7 ordinary differential equations, is formulated and analyzed:

$$\left\{ \begin{array}{l} \frac{dS}{dt} = -\frac{\alpha_I S(t)I(t)}{N} - \frac{\alpha_E S(t)E(t)}{N} + \frac{1}{t_{imm}} R(t), \\ \frac{dE}{dt} = \frac{\alpha_I S(t)I(t)}{N} + \frac{\alpha_E S(t)E(t)}{N} - \frac{1}{t_{inc}} E(t), \\ \frac{dI}{dt} = \frac{1}{t_{inc}} E(t) - \frac{1}{t_{inf}} I(t), \\ \frac{dR}{dt} = \frac{\beta(t)}{t_{inf}} I(t) + \frac{1 - \varepsilon_{HC}}{t_{hosp}} H(t) - \frac{1}{t_{imm}} R(t), \\ \frac{dH}{dt} = \frac{1 - \beta(t)}{t_{inf}} I(t) + \frac{1 - \mu}{t_{crit}} C(t) - \frac{1}{t_{hosp}} H(t), \\ \frac{dC}{dt} = \frac{\varepsilon_{HC}}{t_{hosp}} H(t) - \frac{1}{t_{crit}} C(t), \\ \frac{dD}{dt} = \frac{\mu}{t_{crit}} C(t). \end{array} \right. \quad (2)$$

The model (2) does not take into account the self-isolation index from Yandex, as it has stopped being updated since 2021 due to the removal of restrictive and control measures. The model takes into account:

- incubation period t_{inc} of asymptomatic infection,
- the possibility of re-infection due to weakening of immunity during the time t_{imm} ,
- hospitalization time t_{hosp} and duration of artificial lung ventilation (ALV) device use t_{crit} regulated in the simulated region,
- possible mortality after critical state.

The description of parameters of the model (2) and initial conditions characterizing the spread of COVID-19 in the Novosibirsk region from 31.01.2022 (the period of the outbreak due to the appearance of a new Omicron strain in the region) is given in the table 1.

The spatial SEIR-HCD model [8] of the COVID-19 outbreak propagation is based on the model (2) and is described by a system of reaction-diffusion type equations

$$\left\{ \begin{array}{l} \partial_t s = \nabla(n v_s \nabla s) - \alpha_i s i - \alpha_e s e + t_{imm}^{-1} r, \\ \partial_t e = \nabla(n v_e \nabla e) + \alpha_i s i + \alpha_e s e - t_{inc}^{-1} e, \\ \partial_t i = \nabla(n v_i \nabla i) + t_{inc}^{-1} e - t_{inf}^{-1} i, \\ \partial_t r = \nabla(n v_r \nabla r) + \beta(t) t_{inf}^{-1} i + (1 - \varepsilon_{HC}) t_{hosp}^{-1} h - t_{imm}^{-1} r, \\ \partial_t h = (1 - \beta(t)) t_{inf}^{-1} i + (1 - \mu) t_{crit}^{-1} c - t_{hosp}^{-1} h, \\ \partial_t c = \varepsilon_{HC} t_{hosp}^{-1} h - t_{crit}^{-1} c, \\ \partial_t d = \mu t_{crit}^{-1} c, \end{array} \right. \quad (3)$$

initial conditions

$$\begin{aligned} s(x, 0) &= e^{-(x+1)^4} + e^{-\frac{(x-0.35)^2}{10^{-2}}} + \frac{1}{8} \left(e^{-\frac{(x-0.62)^4}{10^{-5}}} + e^{-\frac{(x-0.52)^4}{10^{-5}}} + e^{-\frac{(x-0.42)^4}{10^{-5}}} \right) + \frac{1}{4} e^{-\frac{(x-0.735)^4}{10^{-5}}}, \\ e(x, 0) &= \frac{1}{20} e^{-\frac{(x-0.75)^4}{10^{-5}}}, \quad i(x, 0) = i_0, \quad r(x, 0) = r_0, \quad h(x, 0) = h_0, \\ c(x, 0) &= c_0, \quad d(x, 0) = d_0, \end{aligned} \quad (4)$$

Table 1: SEIR-HCD model parameters characterizing the distribution of COVID-19 in the Novosibirsk region from 31.01.2022.

Parameter	Description	Value
α_E	Infection parameter for asymptomatic and susceptible groups	0.0922
α_I	Infection parameter for infected and susceptible groups	0.3856
$\beta(t)$	Proportion of individuals with late IgG antibodies to SARS-CoV-2 obtained by Invitro	Data [13]
ε_{HC}	Proportion of hospitalized cases with ALV support	0.0376
μ	Proportion of dead from COVID-19	0.4754
t_{inc}	Incubation period duration (days)	LogN(4.6,4.8)
t_{inf}	Infection period duration (days)	LogN(6.6, 4.9)
t_{hosp}	Hospitalization period duration (days)	LogN(3, 7.4)
t_{crit}	ALV support duration (days)	LogN(6.2, 1.7)
t_{imm}	Average duration of natural immunity (days)	LogN(150, 30)
N	Population of the Novosibirsk region	2798170
S_0	Initial number of susceptible cases	2734917
E_0	Initial number of asymptomatic cases	4329
I_0	Initial number of infected cases	3508
R_0	Initial number of recovered cases	32333
H_0	Initial number of hospitalized cases	219
C_0	Initial number of critically ill cases	54
D_0	Initial number of dead cases	4932

where $u_0 = \frac{U_0}{N}$, and boundary conditions of the form

$$\partial_x u(0, t) = 0, \quad u(1, t) = 0. \quad (5)$$

Here $v = (v_s, v_e, v_i, v_r)$ are the velocities of the groups of susceptible, asymptomatic and infected COVID-19 carriers, and recovered of COVID-19, and $q = (\alpha_i, \alpha_e, \varepsilon_{HC}, \mu)$ is the vector of model parameters characterizing the spread of COVID-19 in a particular region. In this paper, it is assumed that the hospitalized population, critical and dead populations cannot move in space.

The direct problem for the model (3)–(5) in this paper denotes the problem of modelling the COVID-19 propagation process, which requires finding the vector function $u(x, t)$ when v and q are given.

The parameters of the model (3)–(5) are the pair (v, q) , where v is the vector of scalar diffusion parameters with units of 1/(person per day).

1.1 Numerical methods for solving the direct problem

In this section, we present numerical methods for solving the direct initial boundary value problem (3)–(5): finite element method (FEM) and finite difference method (FDM).

1.1.1 Finite element method

For FEM, the computational domain is partitioned into sub-regions called finite elements, within which the function $u(x, t)$ is approximated by selected basis functions.

First we consider a weak formulation of the problem, for this purpose the initial equation is multiplied by the trial function ϕ and integrated over the space. Let us consider the first equation from the system (3) as an example:

$$\int_0^1 \psi \partial_t s dx = \int_0^1 \psi (\nabla \cdot (n v_s \nabla s) - \beta_i s i - \beta_e s e) dx.$$

Integrating by parts the summand with the gradient, we obtain a weak formulation of the problem:

$$\int_0^1 \psi \partial_t s dx = \int_0^1 (-\nabla \psi (n v_s \nabla s) - \psi \beta_i s i - \psi \beta_e s e) dx + \psi n v_s \nabla s|_{x=0}. \quad (6)$$

Linear functions are chosen as basis functions on the element, then trial functions are chosen in correspondence to them:

$$\psi_k = \begin{cases} \frac{x-x_{k-1}}{x_k-x_{k-1}}, & x \in [x_{k-1}, x_k], \\ \frac{x_{k+1}-x}{x_{k+1}-x_k}, & x \in [x_k, x_{k+1}], \\ 0 & , \text{ otherwise.} \end{cases}$$

where $x_i < x_{i+1}$, $i = 0, \dots, N_x$ are the boundaries of the finite elements. Then the solution can be represented as

$$\sum_{k=0}^{N_x} u_k \psi_k,$$

where $u_k = (s_k, e_k, i_k, r_k, h_k, c_k, d_k)$ is the vector of function values at the point x_k at time t . Substituting the functions in this form into equation (6) and replacing the time derivative with a finite-difference analogue, we obtain

$$\int_0^1 \psi_s \psi_k \frac{s_k - s_{k-1}}{\tau} dx = \sum_{k=1}^{N_x-1} \int_0^1 (\nabla \psi_k \nabla \psi_s (n_k v_s s_k) - \psi_s \psi_k \beta_i s_k i_k - \psi_s \psi_k \beta_e s_k e_k) dx + (\psi_s \psi_N n_N v_s \nabla s_N)|_{x=1} - (\psi_s \psi_0 n_0 v_s \nabla s_0)|_{x=0},$$

whence we obtain the values of the local stiffness matrix K , which must be such that

$$[K_j u = -n_k v_s \frac{1}{h} \begin{pmatrix} 1 & -1 \\ -1 & 1 \end{pmatrix} \begin{pmatrix} s_j \\ s_{j+1} \end{pmatrix} - \frac{1}{\tau} \frac{h}{6} \begin{pmatrix} 2 & 1 \\ 1 & 2 \end{pmatrix} \begin{pmatrix} s_j \\ s_{j+1} \end{pmatrix} + \beta_i s_j \frac{h}{6} \begin{pmatrix} 2 & 1 \\ 1 & 2 \end{pmatrix} \begin{pmatrix} i_j \\ i_{j+1} \end{pmatrix} + \beta_e s_j \frac{h}{6} \begin{pmatrix} 2 & 1 \\ 1 & 2 \end{pmatrix} \begin{pmatrix} e_j \\ e_{j+1} \end{pmatrix}].$$

And the right side is calculated as

$$M_j u = -\frac{1}{\tau} \frac{h}{6} \begin{pmatrix} 2 & 1 \\ 1 & 2 \end{pmatrix} \begin{pmatrix} s_j^{t-\tau} \\ s_{j+1}^{t-\tau} \end{pmatrix}.$$

Adding all matrices K_j and right-hand sides, we obtain a system of linear algebraic equations, the solution of which will be the required coefficients u_k .

1.1.2 Finite difference method

The FDM approximates a continuous vector of functions $u(x, t)$ by its grid analogue (u_k^j) . For this purpose, a grid in the closed region $\Omega = \{(x, t) \mid 0 \leq x \leq 1, 0 \leq t \leq T\}$ is introduced:

$$\omega = \{(x_k, t_j) \mid x_k = kh, t_j = j\tau, j = 0, \dots, N_x, k = 0, \dots, N_t\},$$

where $h = \frac{1}{N_x}$ and $\tau = \frac{T}{N_t}$.

Then the first and second derivatives are approximated by finite differences with approximation order $O(\tau + h^2)$, resulting in difference equations

$$\begin{aligned}
\frac{s_k^{j+1} - s_k^j}{\tau} &= v_s \frac{n_{k+1}^j - n_{k-1}^j}{2h_x} \frac{s_{k+1}^j - s_{k-1}^j}{2h_x} + v_s n_k^j \frac{s_{k+1}^j - 2s_k^j + s_{k-1}^j}{h_x^2} - \alpha_i s_k^j i_k^j - \alpha_e s_k^j e_k^j + \\
&\quad + t_{imm}^{-1} r_k^j, \\
\frac{e_k^{j+1} - e_k^j}{\tau} &= v_e \frac{n_{k+1}^j - n_{k-1}^j}{2h_x} \frac{e_{k+1}^j - e_{k-1}^j}{2h_x} + v_e n_k^j \frac{e_{k+1}^j - 2e_k^j + e_{k-1}^j}{h_x^2} + \alpha_i s_k^j i_k^j + \alpha_e s_k^j e_k^j - \\
&\quad - t_{inc}^{-1} e_k^j, \\
\frac{i_k^{j+1} - i_k^j}{\tau} &= v_i \frac{n_{k+1}^j - n_{k-1}^j}{2h_x} \frac{i_{k+1}^j - i_{k-1}^j}{2h_x} + v_i n_k^j \frac{i_{k+1}^j - 2i_k^j + i_{k-1}^j}{h_x^2} + t_{inc}^{-1} e_k^j - t_{inf}^{-1} i_k^j, \\
\frac{r_k^{j+1} - r_k^j}{\tau} &= v_r \frac{n_{k+1}^j - n_{k-1}^j}{2h_x} \frac{r_{k+1}^j - r_{k-1}^j}{2h_x} + v_r n_k^j \frac{r_{k+1}^j - 2r_k^j + r_{k-1}^j}{h_x^2} + \beta(t) t_{inf}^{-1} i_k^j + \\
&\quad + (1 - \varepsilon_{HC}) t_{hosp}^{-1} h_k^j - t_{imm}^{-1} r_k^j, \\
\frac{h_k^{j+1} - h_k^j}{\tau} &= (1 - \beta(t)) t_{inf}^{-1} i_k^j + (1 - \mu) t_{crit}^{-1} c_k^j - t_{hosp}^{-1} h_k^j, \\
\frac{c_k^{j+1} - c_k^j}{\tau} &= \varepsilon_{HC} t_{hosp}^{-1} h_k^j - t_{crit}^{-1} c_k^j, \\
\frac{d_k^{j+1} - d_k^j}{\tau} &= \mu t_{crit}^{-1} c_k^j,
\end{aligned}$$

for $k = 1, \dots, N_x - 1$, $j = 0, \dots, N_t - 1$, and the difference analogues of the initial and boundary conditions are of the form:

$$\begin{aligned}
s_k^0 &= s(x_k, 0), \quad e_k^0 = e(x_k, 0), \quad i_k^0 = i_0, \quad \text{for } k = 0, \dots, N_x, \\
r_k^0 &= r_0, \quad h_k^0 = h_0, \quad c_k^0 = c_0, \quad d_k^0 = d_0, \\
\frac{-3u_0^{j+1} + 4u_1^{j+1} - u_2^{j+1}}{2h} &= 0, \quad \text{for } j = 0, \dots, N_t - 1, \\
u_{N_x}^j &= 0, \quad \text{for } j = 1, \dots, N_t.
\end{aligned}$$

Whence we obtain explicit expressions for the definition of the function u_k^j for all k and j .

2. INVERSE PROBLEM STATEMENT

In the inverse problem for the model (3)–(5), in addition to the function vector $u(x, t)$, the unknowns are the initial functions $s(x, 0)$, $e(x, 0)$, and $i(x, 0)$.

We assume that additional information about the process at K days of measurements and x_i points of potential sources is given, i. e.

$$I(t_k) = I_k, \quad C(t_k) = C_k, \quad D(t_k) = D_k, \quad k = 1, \dots, K. \quad (7)$$

Here I_k , C_k , and D_k are the number of infected, critical, and dead cases on day k , respectively.

The problem of determining the vector of three functions in general form from information of the type (7) is incorrect (i. e., its solution may be non-unique and/or unstable) [14]. Therefore, it is assumed that the number of sources having exponential form (4) (analogue of ‘‘Gaussian cap’’) is known (they can be large centers in regions, cities in the country) and has the form [6]

$$\begin{aligned}
s(x, 0) &= a_1^s e^{-\frac{(x-b_1^s)^4}{c_1^s}} + a_2^s e^{-\frac{(x-b_2^s)^4}{c_2^s}} + a_3^s e^{-\frac{(x-b_3^s)^4}{c_3^s}}, \\
e(x, 0) &= a_1^e e^{-\frac{(x-b_1^e)^4}{c_1^e}} + a_2^e e^{-\frac{(x-b_2^e)^4}{c_2^e}} + a_3^e e^{-\frac{(x-b_3^e)^4}{c_3^e}}, \\
i(x, 0) &= i_0.
\end{aligned}$$

The inverse problem (3)–(5), (7) consists of recovering the parameter vector $q = (a^p, b^p, c^p, i_0)$, $p = \{s, e\}$, model (3) using data I_k , C_k , and D_k of the form (7).

2.1 Variational formulation of the problem

To refine the vector of unknown parameters q , we consider a variational formulation of the inverse problem, which consists of minimizing the quadratic target functional

$$J(q) = \sum_{k=1}^K |I(t_k; q) - I_k|^2 + |C(t_k; q) - C_k|^2 + |D(t_k; q) - D_k|^2. \quad (8)$$

2.2 Sensitivity analysis of the inverse problem parameters

2.2.1 Sobol sensitivity analysis

One of the ways to investigate the sensitivity of a model to unknown parameters is the method based on analysis of variance of the model [15, 16]. These methods are based on the consideration of the distribution of unknown parameters using Monte Carlo methods, the main task of which is to calculate sensitivity indices for each of the parameters under study. Let the model be given in the form

$$Y = f(q_1, \dots, q_k), \quad (9)$$

where q_1, \dots, q_k is the set of unknown parameters. We generate a matrix Q of dimension $N \times (k+2)$, which is a random set of unknown parameters $\vec{q} = q_i, i = 1 \dots k$ in the given unspecified bounds. Then the variance-based first-order effect on the model (9) for parameter q_i can be written as

$$V_{q_i}(E_{\mathbf{Q}_i}(Y|q_i)). \quad (10)$$

Here q_i is the i th parameter, \mathbf{Q}_i is the generated matrix of unknown parameters without q_i . The meaning of the expectation operator $E_{\mathbf{Q}_i}(Y|q_i)$ is that the mean value for Y is taken over all possible values of \mathbf{Q}_i at fixed q_i . At the same time, the variance of V_{q_i} is taken over all possible values of q_i . The corresponding sensitivity measure of parameter q_i (first-order sensitivity coefficient) is written as follows:

$$S_i = \frac{V_{q_i}(E_{\mathbf{Q}_i}(Y|q_i))}{V(Y)}. \quad (11)$$

Here $V(Y)$ is the variance across all rows of the matrix Y . Thus, the sensitivity indices represent the expected reduction in variance that would be obtained if the value of parameter q_i could be fixed, normalised by the total variance.

Details of the software implementation and source code can be found in the documentation <https://salib.readthedocs.io/en/latest/basics.html> and in the paper [17].

For the model (3), an identifiability analysis of the unknown parameters $\vec{q} = (\alpha_i, \alpha_e, t_{inc}, t_{inf}, \beta(t), \varepsilon_{HC}, t_{hosp}, t_{imm}, \mu, t_{crit}, v_s, v_e, v_i, v_r)$ using the Sobol method in the Python implementation of the Salib library <https://github.com/SALib/SALib>.

Figure 2 shows the values of the sensitivity indices S_i for all unknown parameters at different time slices, i. e., the variance of the system at five time points of the direct problem solution was investigated: on the 40th, 80th, 120th, 160th, and 200th days of the simulation.

The graph shows that the parameter t_{imm} becomes more influential for the system with time, which is natural because population immunity increases with time. At the same time, the sensitivity indices of the parameters $\alpha_i, t_{inc}, t_{inf}, t_{hosp}$ on the contrary gradually decrease. This may be due to the specificity of the model: the compartments responsible for the spread of the disease (I, E, H), in whose equations the latter parameters are involved, have a wave-like feature and decay with time (see figure 3).

The figure (4) shows bar charts of the values of sensitivity indices as a function of time. The diagram shows that α_i is the most sensitive parameter, while the parameters v_s, v_i, v_r, v_e are the least sensitive and do not contribute significantly to the variance of the results of the model (3).

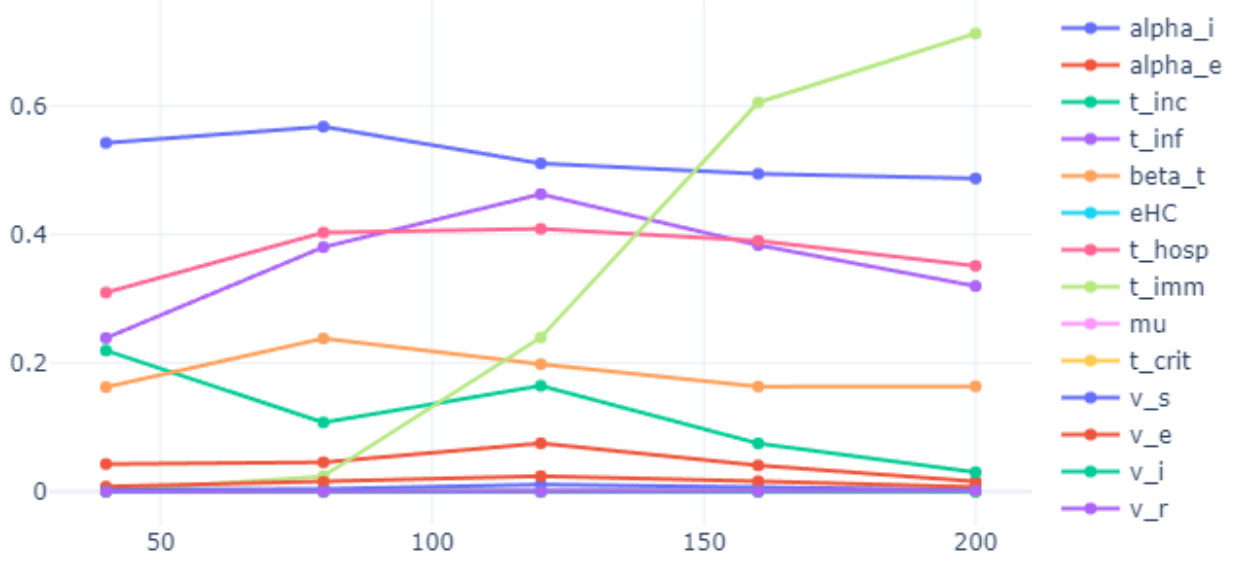


Figure 2: Sensitivity indices for unknown parameters \vec{q} over time. Values are presented for the 40th, 80th, 120th, 160th and 200th days of modelling.

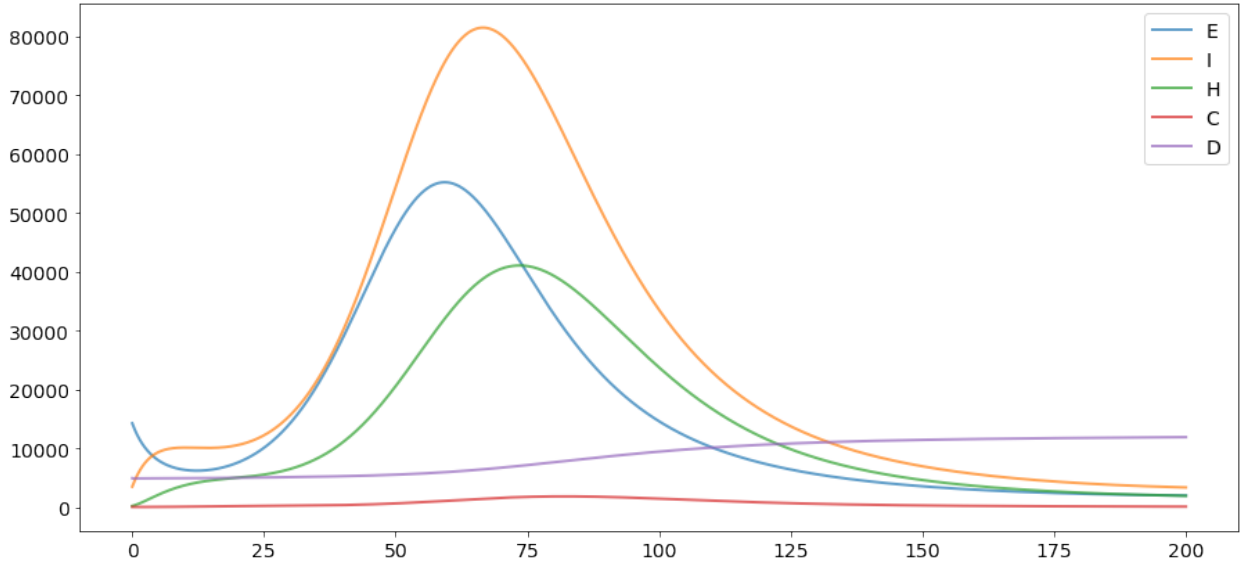


Figure 3: Solution of the direct problem for the model (3) with given parameters $\alpha_i = 0.3856$, $\alpha_e = 0.0922$, $t_{inc} = 5$, $t_{inf} = 8$, $\beta_t = 0.4$, $\epsilon_{HC} = 0.0376$, $t_{hosp} = 7$, $t_{imm} = 175$, $\mu = 0.4754$, $t_{crit} = 9$, $v_s = 5e - 5$, $v_e = 1e - 3$, $v_i = 1e - 10$, $v_r = 5e - 5$.

2.2.2 Method of sensitivity analysis based on Bayesian approach

Another method of investigating the sensitivity of unknown parameters to real data and refining their bounds before searching for optimal values in the course of solving the inverse problem is the method based on the Bayesian approach [18]. Its main idea is to construct a simple hybrid model (emulator) for the model under study (simulator). Due to the feature of the emulator type, it requires much less computational and time resources, so it can be run repeatedly to assess the degree of influence of parameters on the model result.

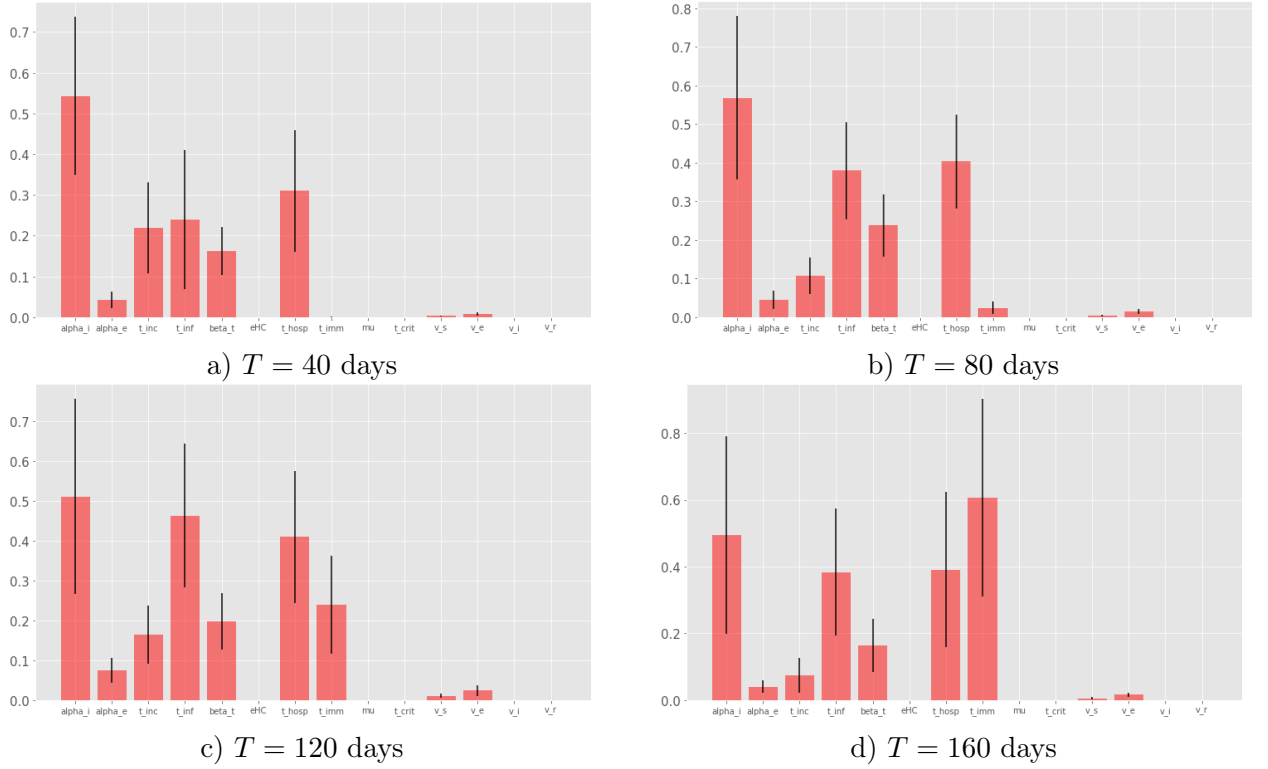


Figure 4: Diagrams of sensitivity index values for unknown parameters \vec{q} for different time slices. The red bars represent the values of indices S_i , the black lines represent the confidence intervals for S_i .

The emulator is the following function of the unknown parameters:

$$g(\vec{q}) = \sum_{i=1}^p h_i(\vec{q}) \cdot \beta_i + u(\vec{q}), \quad (12)$$

where $h_i(\vec{q})$ are monomials of order i , β_i are regression coefficients, $u(\vec{q})$ is a Gaussian process.

The general algorithm for investigating the identifiability of parameters using the emulator is as follows:

1. We specify a set of 250 parameters $\vec{q} = \{q_i | q_i \in [a_i, b_i], i = 1 \dots N\}$ (here N is the number of unknown parameters, $[a_i, b_i]$ is the unspecified bounds for them) using the Latin hypercube [19] for a uniform distribution of points in N -dimensional space.
2. The direct problem (3) is solved 250 times from the unknown parameter values generated in step 1 and the model results are stored.
3. An emulator with zero mean function and exponential correlation function of Gaussian process is created:

$$c(\vec{q}, \vec{q}') = \sigma^2 \cdot \exp \left[- \sum_{i=1}^p \frac{(q_i - q'_i)^2}{\delta_i^2} \right]. \quad (13)$$

4. We implement the selection of β_i parameters of the emulator to match the simulator output data that were obtained in (2). For this purpose, we solve the inverse problem using the quasi-Newtonian L-BFGS-B [20] optimization method.
5. The last step in the analysis is the determination of the parameter indentifiability space, which is carried out using the history matching method. To do this, 50 000 parameter sets are generated and then the emulator outputs at these points are compared to real observations to determine data-driven plausibility bounds. History matching involves the calculation of an

implausibility metric, which establishes how well a particular set of input parameters describes real observations:

$$I(\vec{q}^*) = \frac{|z - E(g(\vec{q}^*))|}{\sqrt{\text{Var}[z - E(g(\vec{q}^*))]}}. \quad (14)$$

Here z is the real observations (statistical data), \vec{q}^* is the parameter set, $E(g(\vec{q}^*))$ is the mean of the emulator.

6. After computing the implausibility metric, the parameter space is divided into two parts based on the threshold value t ($t = 3$ by the rule 3σ [21]). Thus, we are interested in points with $I(\vec{q}) < 3$, which form the boundaries of the plausible space.
7. In the last step of the algorithm, the different bounds for all outputs are crossed.

The sensitivity of the parameters to real data was investigated, and the bounds were refined by constructing an emulator for 14 unknown model parameters (3)

$$\vec{q} = (\alpha_i, \alpha_e, t_{inc}, t_{inf}, \beta(t), \epsilon_{HC}, t_{hosp}, t_{imm}, \mu, t_{crit}, v_s, v_e, v_i, v_r). \quad (15)$$

The following unspecified parameter bounds were passed to the input of the algorithm, in which point simulation using the Latin Hypercube method took place (table 2).

Table 2: Unspecified bounds on the parameters of the model 3 in which sensitivity analyses were performed using emulator construction.

Parameter	Unspecified boundaries
α_i	[0.0; 38.9]
α_e	[0.0; 9.3]
t_{inc}	[0.0; 505.0]
t_{inf}	[0.0; 808.0]
β_t	[0.0; 40.4]
ϵ_{HC}	[0.0; 3.8]
t_{hosp}	[0.0; 707.0]
t_{imm}	[0.0; 17675.0]
μ	[0.0; 48.0]
t_{crit}	[0.0; 909.0]
v_s	[0.0; 0.005]
v_e	[0.0; 0.101]
v_i	[0.0; 0.001]
v_r	[0.0; 0.005]

Real data for Novosibirsk region on the number of hospitalized, recovered and died from COVID-19 were used as measured data to compare the outputs of the emulators. Thus, 3 plausibility spaces were constructed using the algorithm above for each of the statistics, which were overlapped with each other.

Figure 5 shows the result of the study of the sensitivity of unknown parameters to real data (for a more accurate comparison, the investigated boundaries were normalized to the interval [0,1]).

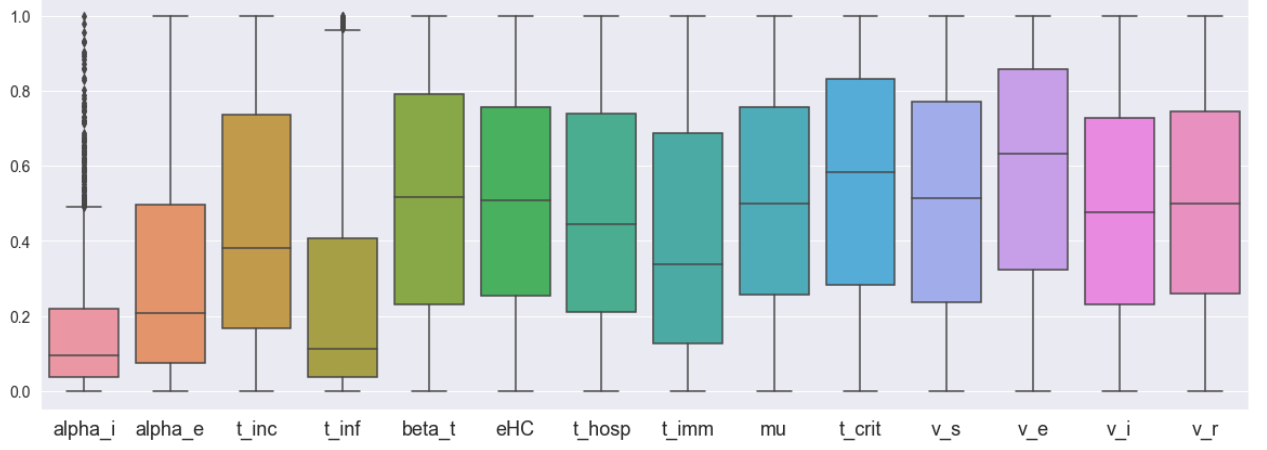


Figure 5: Diagrams of density distributions of unknown parameters in the plausibility space obtained using the Bayesian approach. The boundaries of “boxes with whiskers” represent 25, 50 and 75 quantiles of distributions, the lines at the bottom and top are the unspecified boundaries of unknown parameters.

It can be seen that using this approach, $\alpha_i, \alpha_e, t_{inf}, t_{crit}, t_{imm}$ were selected as the most sensitive parameters, since their 50th quantiles are shifted to one of the specified boundaries, and, accordingly, the points in the plausibility space are densely concentrated in the shifted region. In turn, the other parameters are less sensitive, because for them the points in a plausible space are uniformly distributed, and their refined bounds cannot be specifically determined from real data.

3. ALGORITHM FOR SOLVING INVERSE PROBLEM

The problem of minimizing the target functional (8) is planned to be solved by the Tensor Train (TT) global optimization method [22], the algorithm of which is presented below.

Algorithm of TT method

Require: Lower and upper bounds of the solution space b_{min} and b_{max} , number of parameters (dimensionality of the solution space) d , number of nodes along all directions n , maximum possible rank of wagons r_{max} , number of iterations N_{TT} , initial shift of the functional α , mapping function $h(J(q) - \alpha)$.

- 1: Introduce a mesh with n nodes along each of the d directions.
 - 2: **for** 1 to $d - 1$ **do**
 - 3: Using the grid values and the \hat{q}_{i-1} obtained in the previous step, generate \hat{q}_i .
 - 4: **end for**
 - 5: **while** number of iterations $< N_{TT}$ **do**
 - 6: **for** 1 to $d - 1$ **do**
 - 7: Based on \hat{q}_{i-1} and \hat{q}_i , generate a set of potential solutions M and update the shift α .
 - 8: Remember the best solution q_{best} .
 - 9: Represent the array of values of the function $h(\tilde{q})$, $\tilde{q} \in M$ as a tensor.
 - 10: Compute the tensor approximation in TT format.
 - 11: Using the grid values and \hat{q}_{i-1} , generate \hat{q}_i .
 - 12: **end for**
 - 13: **end while**
-

CONCLUSION

The issue of identifiability of a spatial mathematical model of the spread of fast-moving epidemics based on the law of acting masses and diffusion processes is investigated. The direct problem consists of modelling the COVID-19 spreading process and determining density functions of susceptible, asymptomatic infected, COVID-19 patients, recovered, hospitalized, critical cases requiring artificial lung ventilation and COVID-19 deaths. Algorithms for numerical solution of the direct problem based on finite element method and finite difference method were constructed. The inverse problem, which consists of recovering the vector of parameters characterizing the process of COVID-19 spreading by additional information about the number of identified, critical and dead cases for some period of time, is developed. The algorithm for investigating the issue of model identifiability is based on global methods of Sobol sensitivity analysis and Bayesian approach, which together allowed to reduce the variation boundaries of unknown parameters for further solution of the inverse problem. It is shown that for identification of diffusion coefficients responsible for the rate of movement of individuals in space, it is necessary to use additional information about the process. And also an algorithm for solving the inverse problem based on minimization of the quadratic target functional by the global tensor train optimization method is proposed.

References

- [1] *Kermack W. O., McKendrick A. G.* A contribution to the mathematical theory of epidemics // Proc. Roy. Soc. Lond. A. 1927. V. 115. P. 700–721.
- [2] *Krivorotko O., Kabanikhin S.* Artificial intelligence for COVID-19 spread modeling // J. Inverse Ill-Posed Probl. 2024. V. 32, No. 2. P. 297–332.
- [3] *Krivorotko O. I., Kabanikhin S. I., Zyatkov N. Yu., Prikhodko A. Yu., Prokhoshin N. M., Shishlenin M. A.* Mathematical Modeling and Forecasting of COVID-19 in Moscow and Novosibirsk Region // Num. Anal. Appl. 2020. V. 23, No. 4. P. 332–348.
- [4] *Kolmogorov A. N., Petrovskii I. G., Piskunov N. S.* A study of the diffusion equation with increase in the amount of substance, and its application to a biological problem // Byull. Mosk. Gos. Univ. Mat. Mekh. 1937. V. 1. No. 6. P. 1–26.
- [5] *Murray J. D.* Mathematical Biology. N. Y.: Springer-Verlag, 2007.
- [6] *Viguerie A., Veneziani A., Lorenzo G., Baroli D., Aretz-Nellesen N., Patton A., Yankeelov T., Reali A., Hughes T., Auricchio F.* Diffusion-reaction compartmental models formulated in a continuum mechanics framework: application to COVID-19, mathematical analysis, and numerical study // Comput. Mech. 2020. V. 66. P. 1131–1152.
- [7] *Aristov V. V., Stroganov A. V., Yastrebov A. D.* Simulation of spatial spread of the COVID-19 pandemic on the basis of the kinetic-advection model // Physics. 2021. V. 3, No 1. P. 85–102.
- [8] *Bärwolff G.* A local and time resolution of the COVID-19 propagation — a two-dimensional approach for Germany including diffusion phenomena to describe the spatial spread of the COVID-19 pandemic // Physics. 2021. V. 3, No. 3. P. 536–548.
- [9] *Lau Z., Griffiths I. M., English A., Kaouri K.* Predicting the spatially varying infection risk in indoor spaces using an efficient airborne transmission model // Proc. R. Soc. A. 2022. V. 478, No. 2259. Article 20210383.
- [10] *Boscheri W., Dimarco G., Pareschi L.* Modeling and simulating the spatial spread of an epidemic through multiscale kinetic transport equations // Math. Models Methods Appl. Sci. 2021. V. 31, No. 6. P. 1059–1097.

- [11] *Takács B. M., Faragó I., Horváth R., Repovš D.* Qualitative properties of space-dependent SIR models with constant delay and their numerical solutions // arXiv. 2022. arXiv:2112.06808.
- [12] *Krivorotko O., Zyatkov N.* Data-driven regularization of inverse problem for SEIR-HCD model of COVID-19 propagation in Novosibirsk region // Eurasian J. Math. Comput. Appl. 2022. V. 10, No. 1. P. 51–68.
- [13] <https://ai-biolab.ru/data>
- [14] *Kabanikhin S.* Definitions and examples of inverse and ill-posed problems // J. Inverse Ill-Posed Probl. 2009. V. 16, No. 4. P. 317–357.
- [15] *Cukier R. I., Fortuin C. M., Schuler K. E., Petschek A. G., Schaibly J. H.* Study of the sensitivity of coupled reaction systems to uncertainties in rate coefficients // J. Chem. Phys. 1973. V. 59. P. 3873–3878.
- [16] *Sobol I. M.* Sensitivity analysis for non-linear mathematical models // Math. Model. Comput. Exp. 1993. V. 1. P. 407–414.
- [17] *Saltelli A., Annoni P., Azzini I., Campolongo F., Ratto M., Tarantola S.* Variance based sensitivity analysis of model output. Design and estimator for the total sensitivity index // Comput. Phys. Commun. 2010. V. 180. P. 259–270.
- [18] *Andrianakis I., Vernon I. R., McCreesh N., McKinley T. J., Oakley J. E., Nsubuga R. N., Goldstein M., White R. G.* Bayesian history matching of complex infectious disease models using emulation: a tutorial and a case study on HIV in Uganda // PLoS Comput. Biol. 2015. V. 11. No. 1. Article e1003968.
- [19] *McKay M. D., Beckman R. J., Conover W. J.* A comparison of three methods for selecting values of input variables in the analysis of output from a computer code // Technometrics. 1979. V. 21. P. 239–254.
- [20] *Malouf R.* A comparison of algorithms for maximum entropy parameter estimation // Proc. Sixth Conf. Natur. Lang. Learn. 2002. P. 49–55.
- [21] *Pukelsheim F.* The three sigma rule // Am. Stat. 1994. V. 48. P. 88–91.
- [22] *Zheltkova V. V., Zheltkov D. A., Grossman Z., Bocharov G. A., Tyrtysnikov E. E.* Tensor based approach to the numerical treatment of the parameter estimation problems in mathematical immunology // J. Inverse Ill-Posed Probl. 2018. V. 26. No. 1, P. 51–66.